



## New Sound Absorption Materials: Using Additive Manufacturing for Compact Size, Broadband Sound Absorption at Low Frequencies

Foteini SETAKI<sup>1</sup>; Martin TENPIERIK<sup>1</sup>; Arjan van TIMMEREN<sup>1</sup>; Michela TURRIN<sup>1</sup>

<sup>1</sup> TU Delft, Faculty of Architecture and the Built Environment

### ABSTRACT

Sound absorption systems are widely used for reducing noise and improving room acoustics. However, they are often constrained by conventional design and production techniques; and offer limited options for customising performance and form. Moreover, typical solutions are difficult to use for the damping of low frequencies due to their large size or their narrowband performance.

In response to these limitations, this paper discusses the potential of achieving compact size broadband absorption at lower frequencies, by taking advantage of Additive Manufacturing (AM) technologies. This is addressed by focusing on geometry-related sound absorbing mechanisms with geometrical features that are within the manufacturing capabilities of AM. Two concepts are explored regarding open tube resonant absorbers: (A) a combination of multiple resonators and (B) the introduction of a resistive layer at the resonator's orifice. Each concept is digitally designed and produced with Selective Laser Sintering (SLS). The performance is assessed with a model in Matlab and with measurements in the impedance tube (B&K, type 4206), using the two microphone transfer function method. The results match well with theory on viscothermal wave propagation and show the possibility of targeting low frequencies in compact size.

Keywords: Half-wave resonators, Additive Manufacturing, Sound Absorption

### 1. INTRODUCTION

Sound absorption technologies are broadly used for reducing noise and improving room acoustics. Despite their wide range of applications, they are often constrained by conventional design and production techniques and do not cover the increasing demand in customization, optimized performance and complex shapes. Moreover, typical solutions are difficult to use for the damping of low frequencies due to their large size or their extreme narrowband performance.

These limitations could be addressed by introducing Additive Manufacturing (AM) technologies in the production of sound absorbers. AM enables design freedom and supports the production of complex geometries. This can lead to engineered structures that are designed according to sound absorbing mechanisms and perform better than conventional absorbers. Until now the potentials of the combination of AM with sound absorbing mechanisms were unexplored; to date applications remain limited to prototypes, i.e. (1, 2). However, it is expected that the spread of AM in acoustic applications will increase, due to the fast development and increasing affordability of the technology and the corresponding advantages, such as customization possibilities and material robustness.

This paper investigates the possibility of achieving compact size broadband absorption at low frequencies by focusing on half-wavelength resonators. An advantage of such resonators is that they can act as acoustic filters and yet let mass flow or light pass through (3). Moreover, the performance of such resonators relies mostly on geometrical features such as the length and the diameter of the tube. Hence, it is possible to control acoustic performance through shape and enable the performative design of custom sound absorbing elements. Typically, half-wavelength resonators are characterized by

<sup>1</sup> {f.setaki; m.tenpierik; a.vantimmeren; m.turrin}@tudelft.nl

narrow peaks. Here, it will be shown that the effect of these type of resonators can be improved by: (A) combining multiple resonators, or by (B) introducing a resistive layer at the resonator's orifice. Each concept is digitally designed and produced with Selective Laser Sintering (SLS) and Polyamide (PA12); and assessed with a MatLab model as well as with measurements in the impedance tube (B&K, type 4206).

## 2. METHODS

### 2.1 Theory

This paper reports the results for two 3d-printed samples, which contain tubes with two open ends (Fig. 1). The performance of this type of absorbers relies mainly on the length of the air-path and the radius of its profile. The sound absorbing properties of this resonators can be calculated by using the theory on viscothermal wave propagation in cylindrical tubes as presented by Zwicker and Kosten (5):

$$\mu = \sqrt{\frac{\omega \rho_o R^2}{\eta}} \quad (1)$$

$$B = \sqrt{\frac{\eta \kappa}{\rho_o \nu}} \quad (2)$$

$$K = \frac{\kappa p_o}{1 + \frac{2}{B \mu \sqrt{-j}}} (\kappa - 1) \frac{J_1(B \mu \sqrt{-j})}{J_0(B \mu \sqrt{-j})} \quad (3)$$

$$\rho = \frac{\rho_o}{1 - \frac{2}{\mu \sqrt{-j} J_0(\mu \sqrt{-j})} \frac{J_1(\mu \sqrt{-j})}{\mu \sqrt{-j} J_0(\mu \sqrt{-j})}} \quad (4)$$

With  $\omega$  the angular frequency [ $\text{rad} \cdot \text{s}^{-1}$ ],  $\rho_o$  the mean density [ $\text{kg} \cdot \text{m}^{-3}$ ],  $R$  the radius of the tube [m],  $\eta$  viscosity of air ( $1.84 \times 10^{-5}$  [ $\text{kg}/(\text{m} \cdot \text{s})$ ]),  $\kappa = \frac{c_p}{c_v}$  the ratio of specific heats,  $\nu = \frac{\lambda_n}{\rho_o c_p}$  the reduced thermal conductivity,  $J_0$  and  $J_1$  the Bessel functions of the first kind of order 0 and 1,  $j = \sqrt{-1}$  the imaginary unit. The standard air conditions are:  $c_0 = 343.3$  m/s,  $\rho_o = 1.22$  kg/m<sup>3</sup>,  $p_o = 1.013 \times 10^5$  Pa,  $\lambda_n = 2.41 \times 10^{-2}$  W/mK. The corresponding sound absorption coefficient  $\alpha$ , for a pipe with 2 open ends facing two opposite sides of a wall, is given by (5, 6):

$$\alpha = 1 - \left| \frac{Z - \rho_o c_o}{Z + \rho_o c_o} \right|^2 \quad (5)$$

$$Z = R_m + \sqrt{K \rho} \tanh(j \omega L \sqrt{\frac{\rho}{K}}) \quad (6)$$

$$R_m = R \cdot d \quad (7)$$

With  $d$  the thickness of the porous layer [m],  $Z$  the acoustic impedance and  $L$  the effective length of the resonator consisting of the geometrical length plus two small end corrections  $\Delta L$  at both ends of the resonators.  $\Delta L$  is approximated as  $\frac{8 R_{\text{tube}}}{3 \pi}$ , where  $R_{\text{tube}}$  [m] the radius of the inlet (4).

For pores that are straight cylindrical of radius  $r$  [m], placed parallel to each other, the flow resistivity  $R$  [ $\text{N} \cdot \text{s} \cdot \text{m}^{-4}$ ] can be approximated as (6):

$$R = \frac{16 \eta h (1-h)}{r^2 h^2 [(1-8\Gamma) + 8\Gamma (1-h) - (1-h)^2 - 2 \ln(1-h)]} \quad (8)$$

Where  $\Gamma \approx 0.577$ ,  $h$  the porosity and  $r$  the radius of the pores [m].

For the examined tubes with the two open ends facing the same side of the wall, the resonant frequencies can be calculated based on:

$$f = \frac{(2n-1)c_0}{2L} \quad \text{with, } n = 1, 2, 3, \dots \quad (9)$$

## 2.2 Methods

In open tube resonators, the incident waves are cancelled by the waves in the resonator and damped by the viscothermal losses in the resonator (3). This kind of resonators are usually effective in narrow band noise problems. However, in room acoustics, it is most commonly required to offer solutions that address a wide frequency range. This paper examines two alternatives for achieving larger absorption bandwidth with resonant absorbers by: (A) combining various resonators and, (B) adding a resistive layer at the orifice of the resonator.

By combining resonators -which are tuned for different frequencies- it is possible to absorb noise within a wider frequency band. Sample GP.4.2 examines this concept (Fig. 1); it contains three air-paths with different lengths: 0.343 m (L1), 0.515 m (L2) and 0.686 m (L3). All of them have a constant circular profile with a diameter of 0.015 m. Based on eq. 1, the corresponding design frequencies for n=1 are: 482, 325 and 245 Hz.

To achieve losses, damping is required (7). Often, this is best attained by placing porous absorbers where the particle velocity is large. In this case, as sound is compressed through the holes, the particle velocity is increased at the two orifices of the open tube. Sample GP.3.3.A investigates the effect of adding a resistive layer at the front parts of an open tube in order to gain absorption (Fig. 2). It contains one air-path with two open ends; the air-path has a total length of 0.5213 m and a constant circular diameter of 0.03 m. Based on eq. 1, the first design frequency is expected at 314 Hz (n=1). Two 3d-printed plugs -consisting of small parallel tubes with quadratic profile- are placed at the two open orifices of the tube. The plugs have 0.002 m pore size, 0.03 m thickness and 0.685 porosity. The flow resistivity of the plugs is approximated by using eq. 9 to  $2767.7 \text{ N}\cdot\text{s}\cdot\text{m}^{-4}$ .

The two samples have a thickness of 100 mm, which is up to 10 times smaller than the wavelength of the targeted frequencies. In order to fit the long air-paths in such a small profile, the tubes are bended 5 to 11 times. However, these folds are not expected to affect the results. The fabrication of such a complex geometry is easily possible due to the advances of AM. The bended tubes occupy 65-78% of the total volume of the cylinders. Therefore, there is space for even further reduction of the components' thickness.

Figure 1 shows the prototypes which are produced with Selective Laser Sintering (SLS) from polyamide (PA12). SLS is a powder-based additive manufacturing technique that works by selectively scanning and sintering the surface of the raw-material with a laser. SLS was chosen, among other AM techniques, because of its powder-based nature and its economical and fast features in production. The self-supporting capabilities of the technique allow the fabrication of highly complex internal air paths. Moreover, the post-processing only involves the removal of the unsintered powder using simple techniques such as using compressed air or brushes. Even though the sintered material presents some micro-porosity, it is not expected to affect the measurements. The technique produces parts with high level of accuracy; the small tolerance of  $\pm 0.3\%$  (with a lower limit of  $\pm 0.3 \text{ mm}$ ) is not in the scale that can affect the measurements in the impedance tube.

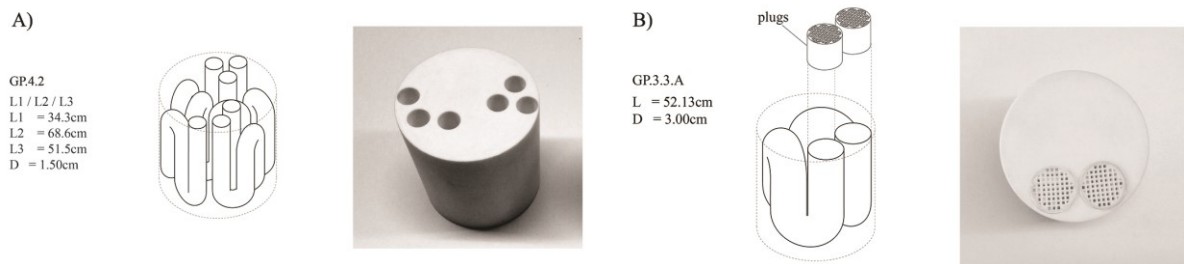


Figure 1 - Samples GP.4.2 (A) and GP3.3 (B) as designed (geometrical features) and as prototyped with SLS and PA12

The sound absorption coefficient of the discussed geometries was measured in the impedance tube (B&K, type 4206); using the two microphone transfer-function method in accordance with NEN EN ISO 10534-2: 2001. This technique is based on the transfer function of two fixed microphones which are placed at two different positions in the impedance tube. The resulting standing wave is build up from a white noise signal. With the measured transfer function the incident and reflected waves are separated mathematically (3). This leads to the reflection coefficient of the sample for the same frequency band as the broadband signal. The impedance and absorption coefficient can be derived as well. The samples were measured 3-5 times each, with different mounting conditions in order to minimise the possibility of experimental error. The transfer function method in combination with 10 cm diameter impedance tube acquires results from 50 to 1600Hz; within this frequency range a 2Hz measurement interval was used. As a final step, the measurements in the impedance tube, are juxtaposed to the results of an analytical model in Matlab that is based on the theory presented in the previous paragraph.

### 3 RESULTS

Figures 3 and 4 show the absorption coefficient ( $\alpha$ ) for normal sound incidence, as measured in the impedance tube and as calculated in Matlab. The results show good agreement with the calculations based on viscothermal wave theory; and the resonance frequencies are predicted well by including the end corrections in the length of the air-paths. Moreover, high absorption peaks are found within certain narrow frequency bands; the corresponding  $\alpha$  values are measured from 0.8 to 1.0 at peak frequencies between 245-1600Hz. As a general remark, the spiky experimental results at low absorption coefficients constitute a minor effect because then the samples act approximately as an acoustically hard surface; in this case the impedance tube is relatively sensitive to measurement errors (3).

For sample GP.4.2, which contains three half-wavelength resonators of different lengths, the transfer function method detects 8 peaks. The resonant frequencies agree well with the analytical model (Fig. 3.A). There are only minor misalignments that relate mostly to the exact  $\alpha$ -value. This might relate to the fact that the 3d-printed material contains small levels of porosity that is not taken into account in the Matlab script. Moreover, the misalignment might relate to model simplifications or to inaccuracies in the measurement or in the prototype. By measuring each tube separately (Fig. 3.B), it is observed that the absorption curve of the total, corresponds to the linear addition of the absorption coefficients of the three single air-paths. Even though the width of the frequency band for each tube is not increased, the combination of multiple tubes -tuned for different frequency sets- shows the possibility of achieving broadband absorption by the “in-line” summation of different resonators. In this case, it is important to adjust the geometry and the layout of the tubes for the desired absorption curve with peak frequencies in smaller intervals.

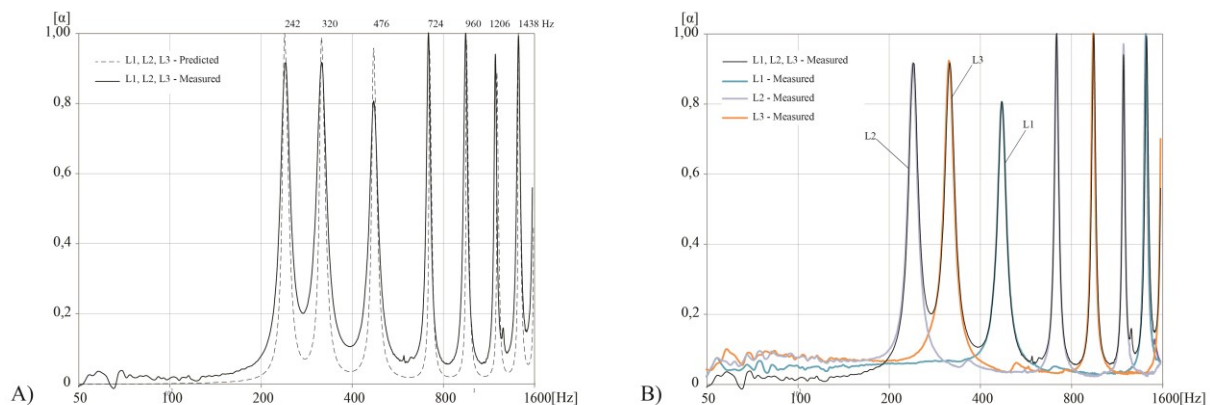


Figure 3: The normal sound absorption coefficient of sample GP.4.2 for: (A) the combination of three air-paths as measured and as calculated and, (B) each air-path separately and for their combination as measured

Sample GP.3.3 is examined with and without the resistive plugs (Fig. 4). The measurements and the predictions are in satisfying agreement. They show that the sample with the plugs performs up to 3 times higher peaks. However, the peaks are not significantly wider. This might be attributed to the low flow resistivity value of the plugs.

Moreover, a small shift of the peaks towards lower frequencies (approx. 25Hz) is observed in the measurements of the sample with the plugs. Possible explanation for this is that the effective length of the air-path is altered due to the resistance insert. Even though, the analytical model predicts the rise of the  $\alpha$ -value well, the shift of the peaks is not anticipated. This might be resolved by including the effect of the tubes in the approximation of the effective length.

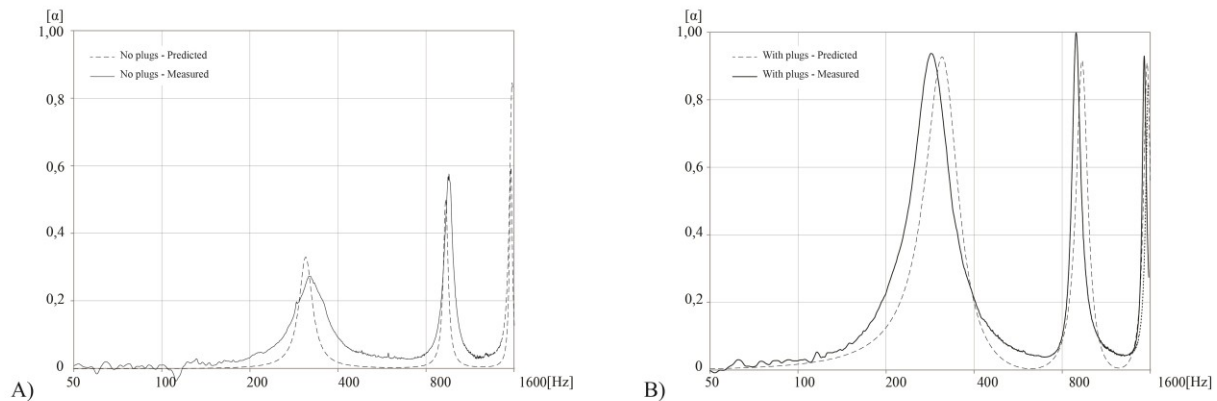


Figure 4: The normal sound absorption coefficient of sample GP.3.3: (A) without resistive plugs as measured and as calculated and, (B) with resistive plugs as measured and as calculated

#### 4 CONCLUSIONS/ DISCUSSION

In this paper, we demonstrated the possibility of producing compact size resonant absorbers for low frequencies by taking advantage of AM. Due to the bending of the tubes, the thickness of the samples became significantly smaller than the corresponding targeted wavelength (approx. 1/10). Moreover, it was shown that the performance of open tube structures can be well predicted based on theory on viscothermal wave propagation. The remaining small discrepancies between the analytical and experimental results may relate to: the material properties of the examined resonators, the inaccuracy during the measurement, the imperfections of the prototype, or the approximation of the effective length of the air-path. Since the Matlab model can predict performance at high levels of accuracy, it may be used as a next step to optimize the sound absorption curve. In this case, the model may need additional parameters, such as the distance between adjacent tubes.

Two concepts were examined for broadband frequency absorption with open-tube resonators: the combination of various tubes and the implementation of a resistive layer at the orifice of the tubes. By combining tubes which are tuned for different frequencies, the resulting absorption coefficient is a linear addition of the two absorption coefficients of the single tubes. In this way, it is possible to achieve broadband sound absorption by simply combining in line suitably tuned resonators.

Furthermore, the covering with the 3d-printed porous plug provides resistance that results in a significant increase of the  $\alpha$ -value. For more effective results in terms of broader frequency band, plugs should be tested with higher flow resistivity values. The control of pore geometry with AM may lead to improvements in tube structures, using only one material and one production technique.

Even though more research needs to be done, the results show good potentials of using AM for achieving compact size, broadband sound absorption at low frequencies.

## ACKNOWLEDGEMENTS

The project is supported by Technology Foundation STW. More partners are involved: Materialise, Peutz, Merford and ARUP. Special thanks to Evert de Ruiter, Diemer de Vries and Lau Nijs.

## REFERENCES

1. Cai XB, Guo QQ, Hu GK, Yang J. Ultrathin low-frequency sound absorbing panels based on coplanar spiral tubes or coplanar Helmholtz resonators. *Appl Phys Lett*. 2014;105(12).
2. Godbold OB, Soar RC, Buswell RA. Implications of solid freeform fabrication on acoustic absorbers. *Rapid Prototyping J*. 2007;13(5):298-303.
3. Eerden, Fvd, Noise reduction with coupled prismatic tubes. University of Twente: Enschede; 2000. 216 Blz. p.
4. Fuchs HV. *Applied Acoustics: Concepts, Absorbers, and Silencers for Acoustical Comfort and Noise Control*. Berlin, Heidelberg: Springer; 2013. Available from: <http://dx.doi.org/10.1007/978-3-642-29367-2>.
5. Kosten CW. *Sound absorbing materials*. New York: Elsevier; 1949. 174 p.
6. Beranek LL, Vér IL. *Noise and vibration control engineering*. 2nd ed. Hoboken: Wiley; 2006. 966 p.
7. Cox TJ, D'Antonio P. *Acoustic absorbers and diffusers : theory, design and application*. 2nd ed. London ; New York: Taylor & Francis; 2009. xvii, 476 p. p.